Submitted to Journal of the
Electrochemical Society

UCRL-20379
Preprint

c.2

RING-DISK AND SECTIONED DISK ELECTRODES

William H. Smyrl and John Newman

December 1970

AEC Contract No. W-7405-eng-48

TWO-WEEK LOAN COPY

This is a Library Circulating Copy
which may be borrowed for two weeks.
For a personal retention copy, call
Tech. Info. Division, Ext. 5545

LAWRENCE RADIATION LABORATORY
UNIVERSITY of CALIFORNIA BERKELEY

UCRL-20379

DISCLAIMER

This document was prepared as an account of work sponsored by the United States Government. While this document is believed to contain correct information, neither the United States Government nor any agency thereof, nor the Regents of the University of California, nor any of their employees, makes any warranty, express or implied, or assumes any legal responsibility for the accuracy, completeness, or usefulness of any information, apparatus, product, or process disclosed, or represents that its use would not infringe privately owned rights. Reference herein to any specific commercial product, process, or service by its trade name, trademark, manufacturer, or otherwise, does not necessarily constitute or imply its endorsement, recommendation, or favoring by the United States Government or any agency thereof, or the Regents of the University of California. The views and opinions of authors expressed herein do not necessarily state or reflect those of the United States Government or any agency thereof or the Regents of the University of California.

UCRL-20379

Ring-Disk and Sectioned Disk Electrodes

William H. Smyrl

Boeing Scientific Research Laboratories,
Seattle, Washington

and

John Newman

Inorganic Materials Research Division,
Lawrence Radiation Laboratory, and
Department of Chemical Engineering,
University of California, Berkeley

December, 1970

Abstract

Integrals relating surface concentration to surface flux for the diffusion layer on a rotating disk are used to evaluate collection efficiencies for a ring-disk system and to assess the error involved in using this system as a sectioned electrode to measure the current distribution. Experimental results are reported which confirm these predictions at the limiting current. Below the limiting current, a nonuniform current distribution is obtained.

Key words: current distribution, collection efficiency

The Diffusion Layer on a Rotating Disk

Equations relating to the diffusion layer on a rotating disk are used to rederive in a new way Albery and Bruckenstein's formula[1] for the collection efficiency of a rotating ring-disk system. The same method is then used to assess the accuracy of using a ring-disk electrode as a sectioned electrode for the direct measurement of the current distribution on a disk electrode.

Steady transfer of a solute species obeys the equation of convective diffusion

$$\underline{v}\cdot\nabla c_i = D_i \nabla^2 c_i \quad , \tag{1}$$

if, for one reason or another, electric migration of this species can be ignored. This condition applies to a neutral solute and to a minor ionic solute in a solution with an excess of inert, supporting electrolyte. The equation also applies to a solution of a single electrolyte where the migration terms can be eliminated by means of the electroneutrality condition.[2-4] In this case, D_i is replaced by the diffusion coefficient of the electrolyte.

The appropriate form of this equation for the diffusion layer on a rotating disk is

$$ay\Omega(\Omega/\nu)^{1/2}\left(r\frac{\partial c_i}{\partial r} - y\frac{\partial c_i}{\partial y}\right) = D_i \frac{\partial^2 c_i}{\partial y^2} \quad . \tag{2}$$

The radial diffusion terms are neglected on the basis of the thinness of the diffusion layer, compared to the radius of the electrode. We treat

the neglect of these terms in a separate paper.[5] For large values of the Schmidt number $Sc = \nu/D_i$, as encountered in electrolytic solutions, the diffusion layer is also much thinner than the hydrodynamic boundary layer, and it is appropriate to approximate the normal and radial components v_y and v_r of the velocity by the first terms of their power-series expansions in the normal distance y from the disk. This introduces the rotation speed Ω, the kinematic viscosity ν, and the dimensionless constant a from the solution of the hydrodynamic problem,[6-8] where it is assumed that the mass-transfer process does not influence the fluid motion.

Equation 2 forms, in essence, the basis of the derivation of the limiting current at a disk electrode.[3,4] It is also the starting point for Newman's analysis of the current distribution on a disk electrode below the limiting current[9] and for Albery and Bruckenstein's analysis of the collection efficiency of a ring-disk system.[1] It is convenient to introduce the dimensionless distance from the disk

$$\zeta = y(a\nu/3D_i)^{1/3} \; (\Omega/\nu)^{1/2} \quad , \tag{3}$$

so that equation 2 becomes

$$3\zeta\left(r\frac{\partial c_i}{\partial r} - \zeta\frac{\partial c_i}{\partial \zeta}\right) = \frac{\partial^2 c_i}{\partial \zeta^2} \quad . \tag{4}$$

The boundary conditions for equation 4 will normally include

$$c_i = c_\infty \text{ at } \zeta = \infty \text{ and } \partial c_i/\partial r = 0 \text{ at } r = 0 \tag{5}$$

as well as a specification of the concentration c_o or the concentration derivative $\partial c_i/\partial\zeta$ or a combination of these on the surface of the disk at $\zeta = 0$. The problem can be solved formally to yield either the derivative at the surface in terms of the surface concentration[10]

$$\left.\frac{\partial c_i}{\partial \zeta}\right|_{\zeta=0} = \frac{-r}{\Gamma(4/3)} \int_o^r \left.\frac{dc_o}{dr}\right|_{r=r'} \frac{dr'}{(r^3-r'^3)^{1/3}} \tag{6}$$

or <u>vice versa</u>[11]

$$c_o(r) - c_\infty = \frac{-1}{\Gamma(2/3)} \int_o^r \left.\frac{\partial c_i}{\partial \zeta}\right|_{\zeta=0} \frac{r'dr'}{(r^3-r'^3)^{2/3}} \tag{7}$$

These equations are analogous to those integral equations commonly used to relate the surface concentration and the normal derivative of concentration for problems involving unsteady, linear diffusion in a stagnant medium. Equation 6 should be regarded as a Stieltjes integral.

Rosner[10,12] has discussed the application of these equations to certain aspects of the ring-disk system and to other geometries (see also Chambré[13] and Chambré and Acrivos[14]). Analogous expressions have been derived for heat-transfer problems by Tribus and Klein.[15] Appendix 2 treats other geometries at high Schmidt numbers.

At the limiting current, the concentration of the reactant is zero over the entire surface of the disk electrode. In equation 6, c_o is regarded in this case to change discontinuously from c_∞ to 0 at $r = 0$, and dc_o/dr is zero over the remainder of the electrode. This equation then yields

$$\left.\frac{\partial c_i}{\partial \zeta}\right|_{\zeta=0} = \frac{c_\infty}{\Gamma(4/3)} \quad , \tag{8}$$

the result of Levich.[3]

Ring and Disk Electrodes

The integrals in equations 6 and 7 can be applied to evaluate the collection efficiency of a ring-disk system and to treat the limiting current on a sectioned disk electrode. We wish to treat three cases.

I. In most applications of rotating ring-disk electrodes, an unstable intermediate is generated on the disk and detected on the ring. The appropriate boundary conditions on the surface are

$$\left.\begin{array}{lll} 0 \leq r \leq r_o & \text{(on the disk)} & c_o = c_d. \\ r_o < r < r_1 & \text{(on the insulating annulus)} & \partial c_i/\partial\zeta = 0. \\ r_1 \leq r \leq r_2 & \text{(on the ring)} & c_o = 0. \end{array}\right\} \tag{9}$$

Here c_d is the concentration of this species on the disk, where it is produced. Normally the bulk value is $c_\infty = 0$. It should be pointed out that the condition of uniform concentration on the disk surface is,

$r_o = 0.25$ cm, $\nu = 0.01$ cm^2/sec, and $D_i = 10^{-5}$ cm^2/sec, the value of this ratio is $(8D_i/9Ar_o^3)^{1/6} = 0.093$.

The fifth boundary condition means that radial diffusion again becomes negligible far downstream in the diffusion layer on the insulator. This condition can be stated more explicitly by obtaining the asymptotic solution for large X. Seek a similarity solution of equation 10 with the term $\partial^2\Theta/\partial X^2$ neglected and subject to the boundary conditions 1 and 4.

$$\Theta \to (9X/2)^{1/3} f(\xi) \text{ as } X \to \infty \quad , \tag{12}$$

where

$$\xi = Y(2/9X)^{1/3} \quad . \tag{13}$$

The function f is found to satisfy the ordinary differential equation

$$f'' + 3\xi^2 f' - 3\xi f = 0 \tag{14}$$

with the boundary conditions

$$f' = 0 \text{ at } \xi = 0 \quad , \quad f \to \xi \text{ as } \xi \to \infty \quad , \tag{15}$$

and the solution

$$f = \xi + \frac{e^{-\xi^3}}{\Gamma(2/3)} - \frac{3\xi}{\Gamma(2/3)} \int_\xi^\infty x e^{-x^3} dx \quad . \tag{16}$$

To effect a numerical solution of the problem for Θ, we used parabolic coördinates in order to avoid infinite derivatives at the

Table 1. Values of c_∞ and c_d for the various cases.

	case	c_d	c_∞
I.	Collection efficiencies	c_d	0
II.	Sectioned disk	0	c_∞
III.	Ring only	c_∞	c_∞

On the disk, the surface flux is given by equation 6.

$$\left.\frac{\partial c_i}{\partial \zeta}\right|_{\zeta=0} = \frac{c_\infty - c_d}{\Gamma(4/3)} \qquad \text{(disk)} \quad . \tag{12}$$

On the insulating annulus, the surface flux is zero. Hence, equation 7 can be used to determine the surface concentration, the surface flux on the disk being given by equation 12.

$$c_o = c_\infty - \frac{c_\infty - c_d}{\Gamma(2/3)\Gamma(4/3)} \int_o^{r_o} \frac{r'dr'}{(r^3 - r'^3)^{2/3}} \quad \text{(annulus)} \ . \tag{13}$$

In appendix 1 it is shown how to evaluate this integral. With that result, equation 13 can be expressed as

$$c_o = c_d + \frac{c_\infty - c_d}{\Gamma(2/3)\Gamma(4/3)} \left[\frac{\pi}{6\sqrt{3}} + \frac{1}{\sqrt{3}} \tan^{-1}\left(\frac{2\theta - 1}{\sqrt{3}}\right) + \frac{1}{6} \ln \frac{(1+\theta)^3}{1+\theta^3}\right] , \tag{14}$$

where

$$\theta^3 = r^3/r_o^3 - 1 \quad . \tag{15}$$

On the ring electrode, the surface concentration is zero, and the surface flux can be obtained from equation 6, the surface

concentration on the disk being given by c_d and the surface concentration on the annulus being given by equation 13 or 14.

$$\left.\frac{\partial c_i}{\partial \zeta}\right|_{\zeta=0} = \frac{-r}{\Gamma(4/3)}\left\{\frac{c_d-c_\infty}{r} + \int_{r_o}^{r_1} \left.\frac{dc_o}{dr}\right|_{r=r'} \frac{dr'}{(r^3-r'^3)^{1/3}} - \frac{c_o(r_1)}{(r^3-r_1^3)^{1/3}}\right\} . \quad (16)$$

From equation 14,

$$\frac{dc_o}{dr} = \frac{c_\infty-c_d}{\Gamma(2/3)\Gamma(4/3)} \frac{r_o^2}{r(r^3-r_o^3)^{2/3}} \quad \text{(annulus)}, \quad (17)$$

and equation 16 becomes

$$\Gamma(\tfrac{4}{3}) \left.\frac{\partial c_i}{\partial \zeta}\right|_{\zeta=0} = c_\infty - c_d + \frac{rc_o(r_1)}{(r^3-r_1^3)^{1/3}}$$

$$- \frac{c_\infty-c_d}{\Gamma(2/3)\Gamma(4/3)} \int_{r_o}^{r_1} \frac{rr_o^2dr'}{r'(r'^3-r_o^3)^{2/3}(r^3-r'^3)^{1/3}} . \quad (18)$$

Let us evaluate a quantity j_r, proportional to the total flow of the species to the ring:

$$j_r = \int_{r_1}^{r_2} \left.\frac{\partial c_i}{\partial \zeta}\right|_{\zeta=0} rdr . \quad (19)$$

Integration of equation 18 in this way over r gives

$$j_r = \frac{1}{2\Gamma(4/3)} \left\{ (c_\infty - c_d)(r_2^2 - r_1^2) + c_o(r_1)(r_2^3 - r_1^3)^{2/3} \right.$$

$$\left. - \frac{(c_\infty - c_d) r_o^2}{\Gamma(2/3)\Gamma(4/3)} \int_{r_o}^{r_1} \frac{(r_2^3 - r'^3)^{2/3} - (r_1^3 - r'^3)^{2/3}}{(r'^3 - r_o^3)^{2/3}} \frac{dr'}{r'} \right\} \quad . \tag{20}$$

In appendix 1 it is shown how to evaluate integrals of the type involved here. Similarly, let

$$j_d = \int_o^{r_o} \left. \frac{\partial c_i}{\partial \zeta} \right|_{\zeta=0} r dr = \frac{c_\infty - c_d}{2\Gamma(4/3)} r_o^2 \quad . \tag{21}$$

In order to avoid writing complicated expressions more than once, let us define N as the following function of the geometric ratios r_2/r_o and r_1/r_o

$$N = \frac{(r_2^3 - r_1^3)^{2/3}}{r_o^2 \Gamma(2/3)\Gamma(4/3)} \int_o^{r_o} \frac{r' dr'}{(r_1^3 - r'^3)^{2/3}} - \frac{r_2^2 - r_1^2}{r_o^2}$$

$$+ \frac{1}{\Gamma(2/3)\Gamma(4/3)} \int_{r_o}^{r_1} \frac{(r_2^3 - r'^3)^{2/3} - (r_1^3 - r'^3)^{2/3}}{(r'^3 - r_o^3)^{2/3}} \frac{dr'}{r'}$$

$$= (A^3 - B^3)^{2/3} \left[\frac{\sqrt{3}}{4\pi} \ln \frac{1+\theta^3}{(1+\theta)^3} - \frac{3}{2\pi} \tan^{-1} \left(\frac{2\theta - 1}{\sqrt{3}} \right) + \frac{3}{4} \right]$$

$$+ \frac{\sqrt{3}}{4\pi} \ln \frac{1 + A^3\psi^3}{(1+A\psi)^3} + \frac{3}{2\pi} \tan^{-1} \left(\frac{2A\psi - 1}{\sqrt{3}} \right) + \frac{1}{4}$$

$$- A^2 \left[\frac{\sqrt{3}}{4\pi} \ln \frac{1+\psi^3}{(1+\psi)^3} + \frac{3}{2\pi} \tan^{-1} \left(\frac{2\psi - 1}{\sqrt{3}} \right) + \frac{1}{4} \right] \quad , \tag{22}$$

where

$$\left.\begin{aligned} A &= r_2/r_o, \quad B = r_1/r_o \quad , \\ \theta &= (B^3-1)^{1/3}, \quad \psi = \frac{1}{A}\left(\frac{A^3-B^3}{B^3-1}\right)^{1/3} \quad . \end{aligned}\right\} \tag{23}$$

Then we can write

$$j_r = -\frac{c_\infty - c_d}{2\Gamma(4/3)} r_o^2 N + \frac{c_\infty (r_2^3 - r_1^3)^{2/3}}{2\Gamma(4/3)} = -j_d N + \frac{c_\infty (r_2^3 - r_1^3)^{2/3}}{2\Gamma(4/3)} \quad . \tag{24}$$

If no other reactions occur, the ratio of the total ring current to the total disk current for the first case in table 1 is found to be

$$-j_r/j_d = N \quad , \tag{25}$$

since in this case $c_\infty = 0$ and all the active intermediate which reacts on the ring is produced at the disk. Then, N is called the collection efficiency, and equation 22 agrees exactly with the expression derived by Albery and Bruckenstein[1] by another method. These authors have tabulated values of N for given values of r_1/r_o and r_2/r_1. The analytic form of the result makes it easy to evaluate N numerically for values of r_1/r_o and r_2/r_1 outside those tabulated.

For case III, where there is no disk electrode, $c_d = c_\infty$, and the total flow to the ring reduces to

$$j_r = c_\infty \frac{(r_2^3 - r_1^3)^{2/3}}{2\Gamma(4/3)} \quad , \tag{26}$$

a result first obtained by Levich[16] and later by Ibl[17] and Rosner.[10]

The geometric quantity N can also be measured with a ring-disk system where both electrodes are operated at the limiting current for the same reaction. Equations 21 and 24 then yield for the ratio of the total ring current to the total disk current, since $c_d = 0$ (case II in table 1),

$$\frac{j_r}{j_d} = \frac{(r_2^3 - r_1^3)^{2/3}}{r_o^2} - N \ , \tag{27}$$

in agreement with the result of Bruckenstein.[18]

The rotating ring-disk electrode system is usually used as a polarographic instrument; species which are generated at the disk are detected on the ring. The presence of unstable intermediates can be detected in this way, but it is difficult to treat quantitatively the kinetics because of uncertainty in the relative importance of ohmic potential drop and concentration and surface overpotentials. On the ring, the influence of surface overpotential and ohmic potential drop is negligible when it is operated at the limiting current. The kinetics of generation of the active intermediate on the disk is less well known, however, because of the nonuniformity of the current distribution on the disk. The assumption of a uniform surface concentration on the disk surface is questionable for case 1 of table 1.

When the ring-disk system is used for plating-type applications, the same reaction would occur on both electrodes, and they would normally be operated at the same potential. If both are operated below

the limiting current, the nonuniform current distribution on the disk again makes it difficult to analyze the electrochemical kinetics. However, it is just because of the nonuniform current distribution that a ring would be used with the disk. The ring-disk system might be used to determine the current distribution, or the ring might be included to make the current distribution more nearly uniform on the disk. Since the nonuniformities are greatest on the outer edge of a disk, the ring might be viewed as "soaking up" the nonuniformities. The justification for use of the ring for either purpose must come from an analysis of the current on a ring as compared to the current over an equivalent area of a disk electrode.

Since sectioned electrodes are commonly used to measure the current distribution on an electrode, frequently at the limiting current, it would be valuable to assess the error introduced by the nonzero thickness of the insulator. One standard of comparison would be the ring current divided by the current density on the disk and the area of the ring electrode. From equation 24, this ratio is given by

$$f_1 = \frac{(r_2^3 - r_1^3)^{2/3} - r_o^2 N}{r_2^2 - r_1^2} \tag{28}$$

and is tabulated in table 2. Departures of this ratio from unity show by how much the average current density on the ring exceeds the current density on the disk. Since limiting currents are being considered, this current density on the disk is the appropriate standard since it would prevail everywhere if the insulating annulus were of zero thickness.

Table 2. Total ring current divided by the current density on the disk and the area of the ring (from equation 28) for the case where both the ring and the disk are at limiting current for the same reaction.

r_2/r_o	1.1	1.2	1.5	2	3
$\frac{r_1^2-r_o^2}{r_2^2-r_1^2}$					
0.05	1.0388	1.0390	1.0395	1.0401	1.0409
0.1	1.0720	1.0724	1.0735	1.0749	1.0767
0.2	1.1304	1.1313	1.1336	1.1366	1.1400
0.5	1.2713	1.2736	1.2795	1.2860	1.2928
1	1.4497	1.4540	1.4641	1.4746	1.4846
2	1.7112	1.7181	1.7337	1.7491	1.7628
5	2.2156	2.2269	2.2514	2.2744	2.2940
10	2.7431	2.7584	2.7910	2.8209	2.8459
20	3.4247	3.4446	3.4869	3.5252	3.5569

As a second standard of comparison, we take the ring current divided by the current density on the disk and the area of both the ring electrode and the insulating annulus. This ratio is given by

$$f_2 = \frac{(r_2^3 - r_1^3)^{2/3} - r_o^2 N}{r_2^2 - r_o^2} \tag{29}$$

and is tabulated in table 3. Again, departures of this ratio from unity show by how much the average current density on the ring and annulus is less than the current density on the disk.

For thin insulators or wide rings, both of these ratios approach unity. For a ring electrode whose area is ten times the area of the insulator, the error represented by the ratio f_2 can be expected to be less than 3 percent while that represented by f_1 can be greater than 7 percent. These ratios thus provide a basis for the design of ring-disk systems for current-distribution studies. Similar considerations apply to the design of sectioned electrodes for other geometries when mass-transfer limitations determine the current distribution (see appendix 2).

The ratio f_2 depends most strongly on the ratio of the area of the insulator to the area of the ring electrode. Consequently, we have used this for one of the geometric parameters in tables 2 and 3. With a strong dependence on this parameter, the choice of the other parameter becomes less important; we chose r_2/r_o, the ratio of the outer radius of the ring to the radius of the disk electrode. These geometric parameters replace the ratios r_1/r_o and r_2/r_1.

Table 3. Total ring current divided by the current density on the disk and the area of both the ring and the annulus (from equation 29) for the case where both the ring and the disk are at limiting current for the same reaction.

r_2/r_o	1.1	1.2	1.5	2	3
$\frac{r_1^2-r_o^2}{r_2^2-r_1^2}$					
0.05	0.9894	0.9895	0.9900	0.9906	0.9914
0.1	0.9746	0.9749	0.9759	0.9772	0.9788
0.2	0.9420	0.9427	0.9447	0.9471	0.9500
0.5	0.8475	0.8491	0.8530	0.8574	0.8619
1	0.7248	0.7270	0.7320	0.7373	0.7423
2	0.5704	0.5727	0.5779	0.5830	0.5876
5	0.3693	0.3712	0.3752	0.3791	0.3823
10	0.2494	0.2508	0.2537	0.2564	0.2587
20	0.1631	0.1640	0.1660	0.1679	0.1694

Experimental Determination of Current Distributions

The experimental investigation of these predictions was divided into two parts. The first objective was to investigate whether or not equation 29 was obeyed at limiting current. The second part was to investigate the departure from this equation below the limiting current, i.e., to determine whether or not a nonuniform current distribution could be observed.

The electrolytic solutions used were composed of KNO_3, $K_4Fe(CN)_6$, and $K_3Fe(CN)_6$. The concentration of KNO_3 was always 1 molar, and the concentrations of the other two components were varied but their ratio was always 1. Fresh, filtered solutions were used for the determinations because it was found that the solutions decompose slowly upon exposure to light and air. The measurements were made at about 23°C.

The rotating ring-disks were constructed of platinum with epoxy insulation. The relevant dimensions of the assemblies were: ring-disk 1(RD1), r_o = 0.441 cm, r_1 = 0.502 cm, r_2 = 0.620 cm and overall radius 1.27 cm; ring-disk 2(RD2), r_o = 0.322 cm, r_1 = 0.478 cm, r_2 = 0.633 cm, and overall radius 1.27 cm; ring-disk 3(RD3), r_o = 0.441 cm, r_1 = 0.498 cm, r_2 = 0.616 cm, and overall radius 1.27 cm. The ring-disks were polished before each run on a metallographic wheel with 0.05μ alumina.

The ring-disks were operated potentiostatically with a Wenking potentiostat. Both were operated anodically. One output from the potentiostat was taken to a parallel circuit in one leg of which was a precision resistor and the connection to the disk, and in the other leg was a variable resistor and the connection to the ring. For measurements at the

limiting current, the potential drop across each resistor was measured, and the current was calculated from this and the measured resistance of each resistor. For measurements below the limiting current, the potential across the resistors was matched to within 0.05 mV. From this and the measured resistance, the current through each resistor was calculated. These potential drops were measured with a Honeywell potentiometric strip chart recorder.

The reference electrode was a strip of platinum partially immersed in a side arm compartment filled with the solution being investigated. The side compartment was connected through a Luggin capillary to the main solution. The capillary tip was positioned in the plane of the disk surface at 2.27 cm from the center of the ring-disk assembly.

The anodic limiting current was attained with overpotentials between +400 mV and +800 mV. In the limiting current region, both the ring current and disk current were constant with potential. In table 4 is listed the ratio of ring current to disk current, in the limiting current region, for each solution used and at several rotation speeds. The results are the average of several runs, and the percent of average deviation is also given. Also given is this ratio multiplied by the ratio of disk area to the area of insulating annulus plus ring electrode. This may be compared to the value of f_2, also listed, calculated from equation 29 .

The experimental results agree with the predictions of equation 29 to better than 1 percent. Also, there is no dependence on concentration or rotation speed, which is also consistent with equation 29 . The deviation from f_2 (theory) is considered to be within experimental error. The largest error was probably the measurement of the electrode dimensions.

Table 4. Sectioned-electrode measurements at limiting current. All solutions were 1 M in KNO_3. Solutions I, II, and III were 0.005, 0.01, and 0.05 M, respectively, in both $K_4Fe(CN)_6$ and $K_3Fe(CN)_6$.

Ring-disk assembly	Solution	Rotation speed (rpm)	$\frac{I_r}{I_d}$	$\frac{I_r}{I_d}\frac{r_o^2}{r_2^2-r_o^2}$	f_2 theory
RD1	I	1550	0.858±0.1%	0.879	0.871
	II	1550	0.852±0.9%	0.872	
	III	1550	0.852±0.1%	0.872	
	III	2500	0.847±0.1%	0.867	
	III	750	0.855±0.1%	0.876	
RD2	I	1550	2.300±0.1%	0.801	0.798
	II	1550	2.308±0.2%	0.804	
	III	1550	2.312±0.2%	0.805	
	III	2500	2.305±0.1%	0.803	
	III	750	2.295±0.5%	0.800	
RD3	III	750	0.832±0.02%	0.875	0.879
	III	1550	0.833±0.3%	0.876	
	III	2500	0.831±0.03%	0.874	

The second part of the investigation, i.e., sectioned electrode measurements below the limiting current, would be expected to reveal a higher value of f_2 (meas.) than predicted by equation 29. This is the result obtained, as shown in figures 1 and 2. Δ is the deviation of the measured results from predictions of equation 29, plotted in figure 1 as a function of the fraction of limiting current on the disk plus ring. Δ is zero at limiting current, and increases with decreasing importance of the concentration overpotential and the increasing importance of ohmic potential drop as the current is decreased below the limiting current.

Curves A and B of figure 1 were obtained for RD2 and RD3 at the same rotation speed in solutions of the same composition. The difference between the two curves is due to the different gap widths of the two assemblies.

Since the outer radii of RD2 and RD3 are approximately equal, curves A and B were obtained with the same value of the dimensionless rotation speed, N, of Newman's theory[9] (not to be confused with the collection efficiency N). This parameter is defined as

$$N = -\Gamma(4/3)\,\frac{ZFr_2 i_{lim}}{RT\,\kappa_\infty}\,.$$

The values of N for curves A and B are* 5.84 and 5.89, respectively. The parameter is a measure of the relative importance of the ohmic potential

*The values of N were calculated from the limiting current density and the conductivity of 1 M KNO_3, i.e., $\kappa_\infty = 0.1\ \mathrm{ohm}^{-1}\mathrm{cm}^{-1}$.

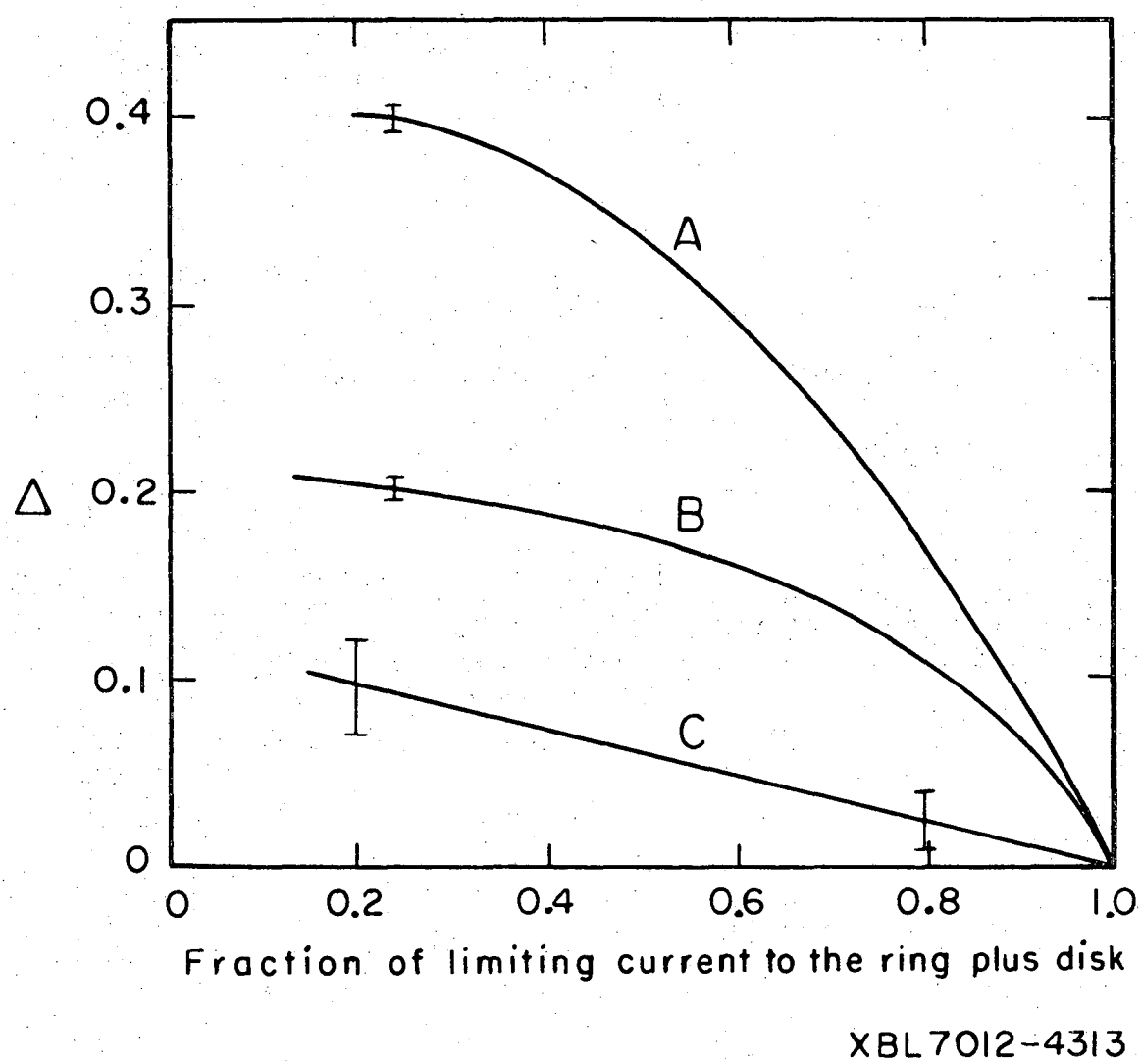

Figure 1. Δ as a function of the fraction of limiting current.
Curve A-RD3, 1550 rpm, 1 M KNO_3, 0.05 M $K_3Fe(CN)_6$, 0.05 M $K_4F_3(CN)_6$.
Curve B-RD2, 1550 rpm, 1 M KNO_3, 0.05 M $K_3Fe(CN)_6$, 0.05 M $K_4Fe(CN)_6$.
Curve C-RD3, 1550 rpm, 1 M KNO_3, 0.005 M $K_3Fe(CN)_6$, 0.005 M $K_4Fe(CN)_6$.
I.- indicates standard deviation.

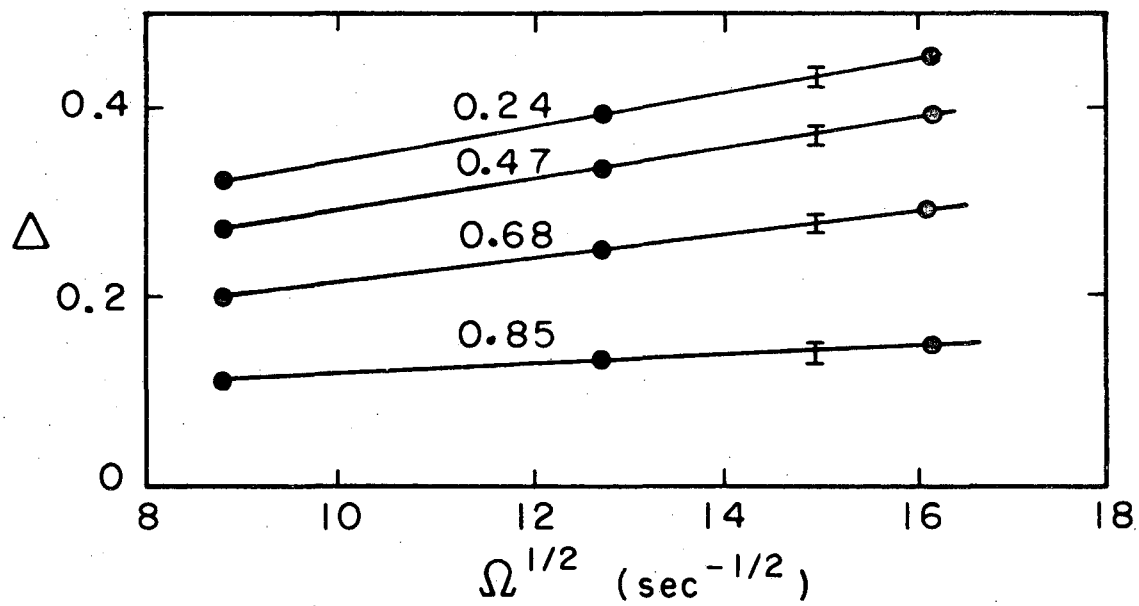

XBL7012- 4312

Figure 2. Δ as a function of rotation speed. Numbers on the curves indicate the fraction of limiting current on ring plus disk. RD3 - 1 M KNO_3, 0.05 M $K_3Fe(CN)_6$, 0.05 M $K_4Fe(CN)_6$. I - indicates standard deviation.

drop as compared to the concentration overpotential at a particular fraction of limiting current.

The effect of changing N was measured in two ways. First, the composition of the solution was changed from 0.05 M in both ferrocyanide and ferricyanide to 0.005 M in both ferrocyanide and ferricyanide. With this solution, the value of N is * 0.595 for RD3, and curve C of figure 1 was obtained. These results may be compared to curve A. Thus, by reducing the concentration of ferro-ferricyanide, one reduces the importance of the ohmic potential drop, at a particular fraction of limiting current, and the current becomes more uniform.

N was also changed by varying the rotation speed, with the results shown in figure 2. The increase of rotation speed increases N and thus the importance of the ohmic drop, producing a less uniform current distribution.

Conclusions

It has been possible to determine the error involved in using the ring-disk system as a sectioned electrode. The predictions for operation at limiting current were verified by experiment within one per cent. When operated below the limiting current, a nonuniform current distribution is observed. The average current density on the ring is higher than the average current density on the disk - an observation which is consistent with Newman's theory.[9]

---

*See footnote on p.19

Bruckenstein and Miller[21] recently reported measurements similar to those here but with a NaBr - $HClO_4$ system. Their measurements also revealed a nonuniform current distribution. They found that an increase in conductivity (thus reducing N) made the current distribution more uniform. They do not report values of the important parameters for their system, nor even the location of the reference electrode, so a more direct comparison with the present results is not possible. It is surprising, however, that the ratio of ring current density to disk current density, which they measure, is constant for various fractions of limiting current (which fractions they do not specify). This should be contrasted with the data reported here, in figure 1. The explanation for this behavior is not clear, but it may be related to the kinetic complications of the NaBr-$HClO_4$ system.[22]

The diffusion coefficient for the ferrocyanide ion in the systems used here has been calculated from the measured anodic limiting currents, and the equation[3,9]

$$i_{lim} = \frac{nFc_\infty}{\Gamma(4/3)} \left(\frac{a}{3}\right)^{1/3} \Omega^{1/2} D_i^{2/3} \nu^{-1/6} \quad .$$

In making the calculations, the viscosity of water and the density of 1 $\underline{M}$ KNO_3 were used. The viscosity of 1 $\underline{M}$ KNO_3, 0.05 $\underline{M}$ ferrocyanide, 0.05 $\underline{M}$ ferricyanide was found to be the same as that for water (within 5 percent) at the same temperature. The results are:

(a) 1 $\underline{M}$ KNO_3, 0.05 $\underline{M}$ $K_3Fe(CN)_6$, 0.05 $\underline{M}$ $K_4Fe(CN)_6$

rotation speeds of 750, 1550, and 2500 rpm

$D_i = 0.567 \times 10^{-5}$ cm^2/sec with a standard deviation of 0.0166×10^{-5} cm^2/sec.

(b) 1 $\underline{M}$ KNO_3, 0.01 $\underline{M}$ $K_3Fe(CN)_6$, 0.01 $\underline{M}$ $K_4Fe(CN)_6$

rotation speed of 1550 rpm

D_i = 0.599 x 10^{-5} cm^2/sec with a standard deviation of 0.007 x 10^{-5} cm^2/sec.

(c) 1 $\underline{M}$ KNO_3, 0.005 $\underline{M}$ $K_3Fe(CN)_6$, 0.005 $\underline{M}$ $K_4Fe(CN)_6$

rotation speed of 1550 rpm

D_i = 0.577 x 10^{-5} cm^2/sec with a standard deviation of 0.013 x 10^{-5} cm^2/sec.

The value of D_i = 0.606 x 10^{-5} cm^2/sec is predicted from the correlation of Gordon, Newman, and Tobias.[23] This compares favorably with that reported here.

The theoretical results for sectioned electrodes can be extended to a variety of geometries involving forced, laminar convection, as shown in appendix 2.

Appendix 1.

First let us evaluate the integral

$$\int_0^x \frac{xdx}{(1-x^3)^{2/3}} = \int_0^1 \frac{xdx}{(1-x^3)^{2/3}} - \int_x^1 \frac{xdx}{(1-x^3)^{2/3}} \quad . \tag{30}$$

In the first integral, make the substitution $y = x^3$; in the second, make the substitution

$$\theta^3 = 1/x^3 - 1 \quad . \tag{31}$$

Then we have

$$\int_0^x \frac{xdx}{(1-x^3)^{2/3}} = \frac{1}{3}\int_0^1 \frac{dy}{y^{1/3}(1-y)^{2/3}} - \int_0^\theta \frac{d\theta}{1+\theta^3}$$

$$= \frac{1}{3}\Gamma(\tfrac{2}{3})\Gamma(\tfrac{1}{3}) - \frac{1}{3}\int_0^\theta \frac{d\theta}{1+\theta} - \frac{1}{3}\int_0^\theta \frac{2-\theta}{\theta^2-\theta+1}\, d\theta$$

$$= \Gamma(\tfrac{2}{3})\Gamma(\tfrac{4}{3}) - \frac{1}{3}\ln(1+\theta) + \frac{1}{6}\ln(\theta^2-\theta+1) - \frac{1}{\sqrt{3}}\tan^{-1}\frac{2\theta-1}{\sqrt{3}}\Bigg|_0^\theta$$

$$= \Gamma(\tfrac{2}{3})\Gamma(\tfrac{4}{3}) + \frac{1}{6}\ln\frac{1+\theta^3}{(1+\theta)^3} - \frac{1}{\sqrt{3}}\tan^{-1}\frac{2\theta-1}{\sqrt{3}} - \frac{\pi}{6\sqrt{3}} \quad . \tag{32}$$

Next we want to evaluate the integral

$$I = \int_1^x \frac{(A^3-x^3)^{2/3}}{(x^3-1)^{2/3}}\,\frac{dx}{x} \quad , \tag{33}$$

where $A \geq x > 1$. Let

$$\omega = x^3/(x^3-1). \tag{34}$$

Then

$$I = \frac{A^2}{3}\int_{\omega}^{\infty} \frac{(\beta\omega-1)^{2/3}d\omega}{\omega(\omega-1)} = \frac{A^2}{3}\left[\int_{\omega}^{\infty} \frac{d\omega}{\omega(\beta\omega-1)^{1/3}} - (1-\beta)\int_{\omega}^{\infty} \frac{d\omega}{(\omega-1)(\beta\omega-1)^{1/3}}\right], \tag{35}$$

where

$$\beta = 1 - 1/A^3 \quad . \tag{36}$$

In the first integral, let $y^3 = \beta\omega - 1$; in the second integral, let $y^3 = (\beta\omega-1)/(1-\beta)$. Then we have

$$I = A^2\int_{\psi}^{\infty} \frac{ydy}{1+y^3} - \int_{A\psi}^{\infty} \frac{ydy}{1+y^3} \quad , \tag{37}$$

where

$$\psi = (\beta\omega-1)^{1/3} = \frac{1}{A}\left(\frac{A^3-x^3}{x^3-1}\right)^{1/3} \quad . \tag{38}$$

The integrals here can now be evaluated in a manner used above for the first integral:

$$I = (A^2-1)\int_{o}^{\infty} \frac{ydy}{1+y^3} + \int_{o}^{A\psi} \frac{ydy}{1+y^3} - A^2\int_{o}^{\psi} \frac{ydy}{1+y^3}$$

$$= (A^2-1)\Gamma(4/3)\Gamma(2/3)$$

$$+ \frac{1}{6}\ln\frac{1+A^3\psi^3}{(1+A\psi)^3} + \frac{1}{\sqrt{3}}\tan^{-1}\left(\frac{2A\psi-1}{\sqrt{3}}\right) + \frac{\pi}{6\sqrt{3}}$$

$$-A^2\left[\frac{1}{6}\ln\frac{1+\psi^3}{(1+\psi)^3}+\frac{1}{\sqrt{3}}\tan^{-1}\left(\frac{2\psi-1}{\sqrt{3}}\right)+\frac{\pi}{6\sqrt{3}}\right] \quad . \tag{39}$$

Note that

$$\Gamma(2/3)\Gamma(4/3) = 2\pi/3\sqrt{3} \tag{40}$$

and that

$$\tan^{-1}\left(\frac{2\psi-1}{\sqrt{3}}\right) = \frac{\pi}{3} - \tan^{-1}\left(\frac{2/\psi-1}{\sqrt{3}}\right) \quad . \tag{41}$$

Appendix 2. Diffusion layers in laminar forced convection at high Schmidt numbers

Because the diffusion coefficient is so small in electrolytic solutions, the diffusion layer generally lies very close to the electrode surface and it is appropriate to approximate the velocity components by the first terms in their power-series expansions in the normal distance from the surface. The Lighthill transformation[19,20] is useful for treating such diffusion layers. The diffusion-layer form of equation 1 then is

$$y\beta\frac{\partial c_i}{\partial x} - \frac{1}{2}\, y^2\, \frac{(\mathcal{R}\beta)'}{\mathcal{R}}\, \frac{\partial c_i}{\partial y} = D_i\, \frac{\partial^2 c_i}{\partial y^2} \quad , \tag{42}$$

where the coördinate system is indicated in figure 3, $\beta(x)$ is the velocity derivative $\partial v_x/\partial y$ at $y = 0$, and for an axisymmetric body $\mathcal{R}(x)$ is the distance of the surface from the axis of symmetry. For two-dimensional diffusion layers, $\mathcal{R} = 1$. Outside the diffusion layer, at $y = \infty$, the concentration is $c_i = c_\infty$.

We solve the problem first for the boundary conditions on the surface

$$\left.\begin{aligned} c_i &= c_\infty \text{ at } y = 0,\ x < x_o. \\ c_i &= 0 \text{ at } y = 0,\ x \geq x_o. \end{aligned}\right\} \tag{43}$$

In terms of the similarity variable

$$\xi = y\sqrt{\mathcal{R}\beta}/[9D_i \int_{x_o}^{x} \mathcal{R}\sqrt{\mathcal{R}\beta}\, dx]^{1/3} \quad , \tag{44}$$

the solution is (for $x > x_o$)

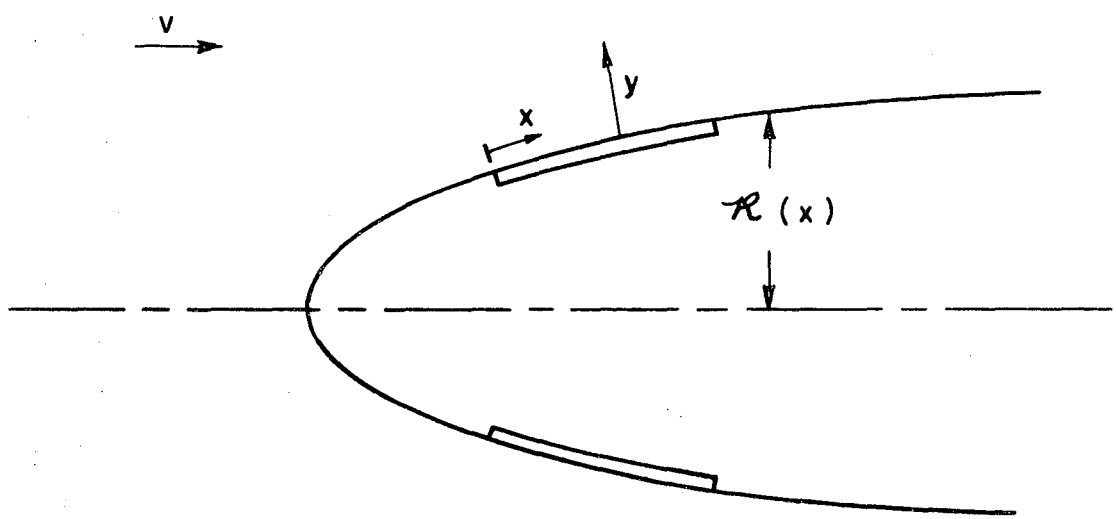

XBL7012-4314

Figure 3. An electrode on an axisymmetric body with axisymmetric flow.

$$\frac{c_i}{c_\infty} = \Theta(\xi) = \frac{1}{\Gamma(4/3)} \int_0^{\xi} e^{-x^3} dx \quad , \tag{45}$$

which gives for the concentration derivative at the wall

$$\left.\frac{\partial c_i}{\partial y}\right|_{y=0} = \frac{c_\infty \sqrt{R\beta}}{\Gamma(4/3)} \Bigg/ \left[9D_i \int_{x_o}^{x} R\sqrt{R\beta}\, dx \right]^{1/3} \quad . \tag{46}$$

The above solution can be used to treat the case of a varying surface concentration by superposition of results for appropriate changes in the surface concentration at many points x_o along the surface:

$$\left.\frac{\partial c_i}{\partial y}\right|_{y=0} = - \frac{\sqrt{R\beta}}{\Gamma(4/3)} \int_0^{x} \left.\frac{dc_o}{dx}\right|_{x=x_o} \frac{dx_o}{\left[9D_i \int_{x_o}^{x} R\sqrt{R\beta}\, dx \right]^{1/3}} \quad . \tag{47}$$

By means of the coordinate transformation

$$r^3 = \int_0^{x} R\sqrt{R\beta}\, dx \text{ and } \zeta = y\sqrt{R\beta} \Bigg/ \left[9D_i \int_0^{x} R\sqrt{R\beta}\, dx \right]^{1/3} \quad , \tag{48}$$

equation 47 becomes

$$\left.\frac{\partial c_i}{\partial \zeta}\right|_{\zeta=0} = \frac{-r}{\Gamma(4/3)} \int_0^{r} \left.\frac{dc_o}{dr}\right|_{r=r'} \frac{dr'}{(r^3-r'^3)^{1/3}} \quad , \tag{49}$$

which is the same as equation 6. The coördinate transformation 48 also reduces equation 42 to equation 4.

Equation 49 should have the same inverse 7 as equation 6. We can derive this in a more straightforward manner than that used in reference 11 by following Tribus and Klein,[15] p. 215. Write equation 49 as

$$\left.\frac{\partial c_i}{\partial \zeta}\right|_{\substack{\zeta=0\\ r=r'}} = \frac{-r'}{\Gamma(4/3)} \int_0^{r'} \left.\frac{dc_o}{dr}\right|_{r=x} \frac{dx}{(r'^3-x^3)^{1/3}} \quad . \tag{50}$$

Multiply by $(r^3-r'^3)^{-2/3}\ 3r'dr'$ and integrate from 0 to r.

$$3\int_0^r \left.\frac{\partial c_i}{\partial \zeta}\right|_{\zeta=0} \frac{r'dr'}{(r^3-r'^3)^{2/3}} = -\int_0^r \frac{3r'^2}{\Gamma(4/3)} \int_0^{r'} \left.\frac{dc_o}{dr}\right|_{r=x} \frac{dx}{(r'^3-x^3)^{1/3}} \frac{dr'}{(r^3-r'^3)^{2/3}} \quad . \tag{51}$$

Interchange the order of integration on the right.

$$3\int_0^r \left.\frac{\partial c_i}{\partial \zeta}\right|_{\zeta=0} \frac{r'dr'}{(r^3-r'^3)^{2/3}} = \frac{-1}{\Gamma(4/3)} \int_0^r \left.\frac{dc_o}{dr}\right|_{r=x} \int_x^r \frac{3r'^2dr'}{(r'^3-x^3)^{1/3}(r^3-r'^3)^{2/3}}\, dx \quad . \tag{52}$$

In the inner integral, let

$$y = (r'^3-x^3)/(r^3-x^3)$$

so that

$$\int_x^r \frac{3r'^2dr'}{(r'^3-x^3)^{1/3}(r^3-r'^3)^{2/3}} = \int_0^1 \frac{dy}{y^{1/3}(1-y)^{2/3}} = \Gamma(\tfrac{1}{3})\Gamma(\tfrac{2}{3}) = \frac{2\pi}{\sqrt{3}} \quad . \tag{53}$$

Then we have

$$\int_0^r \frac{dc_o}{dr}\bigg|_{r=x} dx = c_o(r) - c_\infty = \frac{-1}{\Gamma(2/3)} \int_0^r \frac{\partial c_i}{\partial \zeta}\bigg|_{\zeta=0} \frac{r'dr'}{(r^3-r'^3)^{2/3}} , \qquad (54)$$

in agreement with equation 7. The inverse of equation 47 can thus be written, expressing the surface concentration as an integral over the flux:

$$c_o(x) - c_\infty = - \frac{(D_i/3)^{1/3}}{\Gamma(2/3)} \int_0^x \frac{\partial c_i}{\partial y}\bigg|_{\substack{y=0\\x=x_o}} \frac{\mathcal{R}(x_o)dx_o}{\left[\int_{x_o}^{x} \mathcal{R}\sqrt{\mathcal{R}\beta}\, dx\right]^{2/3}} . \qquad (55)$$

With these results we can now work, for various geometries, the same problems as outlined in table 1. The collection efficiency problem may then not be realistic since we have no justification for assuming that the surface concentration is uniform on the first electrode (<u>unless</u> the first electrode is at limiting current for the reaction which produces the active intermediate). The third problem is trivial since we worked it out before the superposition (see equation 46).

Let us have two electrodes given by

$$0 \le r \le r_o \quad \text{and} \quad r_1 \le r \le r_2,$$

with an insulator between ($r_o < r < r_1$). On the first electrode, $c_o = c_d$, and equation 12 gives the flux. On the insulator, $\partial c_i/\partial\zeta = 0$ at $\zeta = 0$, and the surface concentration is given by equation 13 or 14. On the second electrode, $c_o = 0$, and the flux is given by equation 18.

Note that

$$j_r = \int_{r_1}^{r_2} \left.\frac{\partial c_i}{\partial \zeta}\right|_{\zeta=0} r dr = \left(\frac{D_i}{3}\right)^{1/3} \int_{x_1}^{x_2} \left.\frac{\partial c_i}{\partial y}\right|_{y=0} \mathcal{R} dx \tag{56}$$

and is proportional to the total flow to the second electrode. Similarly, j_d is proportional to the total flow to the first electrode, and equations 21 and 24 apply.

Furthermore, for sectioned electrodes at the limiting current, f_1 anf f_2 have the meaning originally intended (but not stated explicitly). f_1 is the current to the second electrode divided by the current which would flow to the area of the second electrode if the insulator were an electrode. f_2 is the current to the second electrode divided by the current which would flow to the combined area of the second electrode and the insulator if the insulator were an electrode.

Consider the special case of sectioned electrodes in the wall of a flow channel (or a tube or an annulus). $\beta = \beta_o$, a constant, and R is a constant. Then, according to equation 48,

$$r^3 = x\mathcal{R}\sqrt{\mathcal{R}\beta_o} \quad . \tag{57}$$

Tables 2 and 3 still apply, but $A = r_2/r_o = (x_2/x_o)^{1/3}$ and $B = r_1/r_o = (x_1/x_o)^{1/3}$, and the parameters on those tables are

$$\frac{r_2}{r_o} = \left(\frac{x_2}{x_o}\right)^{1/3} \quad \text{and} \quad \frac{r_1^2-r_o^2}{r_2^2-r_1^2} = \frac{x_1^{2/3}-x_o^{2/3}}{x_2^{2/3}-x_1^{2/3}} \quad . \tag{58}$$

Acknowledgment

This work was supported by the United States Atomic Energy Commission and by Boeing Scientific Research Laboratories.

We wish to acknowledge the help of Robert L. Lee of BSRL in making the experimental measurements.

Nomenclature

$a = 0.51023$.

$A = r_2/r_o$.

$B = r_1/r_o$.

c_i - concentration of the species of interest (mole/cm^3).

c_o - surface concentration of the species of interest (mole/cm^3).

c_∞ - concentration of the species of interest outside the diffusion layer (mole/cm^3).

c_d - uniform concentration of the species of interest near the surface of the disk electrode (mole/cm^3).

D_i - diffusion coefficient of the species of interest (cm^2/sec).

f_1 - see equation 28.

f_2 - see equation 29.

i_{lim} - limiting current density on disk electrode (A/cm^2).

I - see equation 33.

j_d - proportional to the total mass-transfer rate to disk electrode (mole/cm).

j_r - proportional to total mass-transfer rate to ring electrode (mole/cm).

N - dimensionless limiting current density for disk electrode (see reference 9).

N - collection efficiency for ring-disk system.

r - radial distance from the axis of the disk.

r_o - radius of disk electrode (cm).

r_1 - inner radius of ring electrode (cm).

r_2 - outer radius of ring electrode (cm).

$\mathcal{R}$ - distance of axisymmetric surface from axis of symmetry (cm).

$Sc = \nu/D_i$, the Schmidt number.

$\underline{v}$ - fluid velocity (cm/sec).

x - distance along electrode (cm).

y - normal distance from the electrode surface (cm).

β - velocity derivative at the wall (sec^{-1}).

Γ - gamma function.

ζ - dimensionless normal distance for the diffusion layer (see also equation 48).

$\theta = (r^3/r_o^3-1)^{1/3}$.

$\theta = (B^3-1)^{1/3}$.

κ_∞ - solution conductivity outside the diffusion layer (mho/cm).

ν - kinematic viscosity (cm^2/sec).

ξ - see equation 44.

ψ - see equation 23.

Ω - rotation speed (radian/sec).

References

1. W. J. Albery and S. Bruckenstein. "Ring-Disc Electrodes. Part 2. -- Theoretical and Experimental Collection Efficiencies." Transactions of the Faraday Society, 62, 1920-1931 (1966).

2. W. Nernst. "Zur Kinetik der in Lösung befindlichen Körper." Zeitschrift für physikalische Chemie, 2, 613-637 (1888).

3. V. Levich. "The Theory of Concentration Polarization." Acta Physicochimica U.R.S.S., 17, 257-307 (1942).

4. John Newman. "Transport Processes in Electrolytic Solutions." Advances in Electrochemistry and Electrochemical Engineering, 5, 87-135 (1967).

5. William H. Smyrl and John Newman. "Limiting Current on a Rotating Disk with Radial Diffusion." November, 1970. UCRL-20378.

6. Th. v. Kármán. "Über laminare und turbulente Reibung." Zeitschrift für angewandte Mathematik und Mechanik, 1, 233-252 (1921).

7. W. G. Cochran. "The flow due to a rotating disc." Proceedings of the Cambridge Philosophical Society, 30, 365-375 (1934).

8. E. M. Sparrow and J. L. Gregg. "Heat Transfer From a Rotating Disk to Fluids of any Prandtl Number." Journal of Heat Transfer, 81C, 249-251 (1959).

9. John Newman. "Current Distribution on a Rotating Disk below the Limiting Current." Journal of the Electrochemical Society, 113, 1235-1241 (1966).

10. Daniel E. Rosner. "Reaction Rates on Partially Blocked Rotating Disks -- Effect of Chemical Kinetic Limitations." Journal of the Electrochemical Society, 113, 624-625 (1966).

11. John Newman. "The Diffusion Layer on a Rotating Disk Electrode." Journal of the Electrochemical Society, 114, 239 (1967).

12. Daniel E. Rosner. "Convective Diffusion Limitations on the Rates of Chemical Reactions at Solid Surfaces -- Kinetic Implications." Eleventh Symposium (International) on Combustion, pp. 181-194 (1967).

13. Paul L. Chambré. "On Chemical Surface Reactions in Hydrodynamic Flows." Applied Scientific Research, 6A, 97-113 (1956).

14. Paul L. Chambré and Andreas Acrivos. "On Chemical Surface Reactions in Laminar Boundary Layer Flows." Journal of Applied Physics, 27, 1322-1328 (1956).

15. Myron Tribus and John Klein. "Forced Convection from Nonisothermal Surfaces." Heat Transfer -- a Symposium, pp. 211-235. Ann Arbor: Engineering Research Institute, University of Michigan, 1953.

16. Veniamin G. Levich. Physicochemical Hydrodynamics, section 18. Englewood Cliffs, N. J.: Prentice-Hall, Inc., 1962.

17. N. Ibl. "Discussion" (of Dissolution of Copper in Sulfuric Acid Solutions by D. P. Gregory and A. C. Riddiford). Journal of the Electrochemical Society, 108, 610 (1961).

18a. S. Bruckenstein. "O sootnoshenii mezhdy predel'nymi tokami diffuzii na vrashchayushchikhsya diskovom, kol'tsevom i kol'tsevom diskovom elektrodakh." Elektrokhimiya, 2, 1085-1088 (1966).

18b. D. T. Napp, D. C. Johnson, and Stanley Bruckenstein. "Simultaneous and Independent Control of Two Indicator Electrodes. Applications to the Copper (II)/Copper (I)/Copper System in 0.5 M KCl at the Rotating Ring-Disc Electrode." Analytical Chemistry, 39, 481-485 (1967).

19. M. J. Lighthill. "Contributions to the theory of heat transfer through a laminar boundary layer." Proceedings of the Royal Society, A202, 359-377 (1950).

20. John Newman. "Engineering Design of Electrochemical Systems." Industrial and Engineering Chemistry, 60 (no. 4), 12-27 (April, 1968).

21. Stanley Bruckenstein and Barry Miller. "An Experimental Study of Nonuniform Current Distribution at Rotating Disk Electrodes." Journal of the Electrochemical Society, 117, 1044-1048 (1970).

22. William H. Smyrl and John Newman. "Detection of Non-uniform Current Distributions on a Disk Electrode." February, 1971. UCRL-20380.

23. Stanley L. Gordon, John S. Newman, and Charles W. Tobias. "The Role of Ionic Migration in Electrolytic Mass Transport; Diffusivities of $[Fe(CN)_6]^{3-}$ and $[Fe(CN)_6]^{4-}$ in KOH and NaOH Solutions." Berichte der Bunsengesellschaft für physikalische Chemie, 70, 414-420 (1966).

LEGAL NOTICE

This report was prepared as an account of work sponsored by the United States Government. Neither the United States nor the United States Atomic Energy Commission, nor any of their employees, nor any of their contractors, subcontractors, or their employees, makes any warranty, express or implied, or assumes any legal liability or responsibility for the accuracy, completeness or usefulness of any information, apparatus, product or process disclosed, or represents that its use would not infringe privately owned rights.

TECHNICAL INFORMATION DIVISION
LAWRENCE RADIATION LABORATORY
UNIVERSITY OF CALIFORNIA
BERKELEY, CALIFORNIA 94720